Study on Indium Composition-Related Leakage Current Behavior Through Analysis of Spatial Electroluminescence Inhomogeneity in Blue and Green Micro Light-Emitting Diodes

Youngwook Shin, Jinchan Seo* and Jaekyun Kim**

***Department of Photonics and Nanoelectronics, Hanyang University, Hanyang daehak-ro 55, Ansan, 15588, Republic of Korea**

jaekyunkim@hanyang.ac.kr

Abstract

Electroluminescence EL spectra are investigated by use of a confocal scanning optical microscopy for InGaN-based blue and green micro-sized light-emitting diodes (μLEDs) to correlate nanoscale emission and macroscopic electrical characteristics. The study reveals that the inhomogeneity in the emission wavelength of green μLEDs, compared to blue μLEDs, is linked to their relatively lower leakage current due to suppressed lateral diffusion and non-radiative recombination at the sidewall.

Author Keywords

Micro-LEDs; Micro spectroscopy; Sidewall damage

1. Introduction

Gallium nitride (GaN)-based micro-scale light-emitting diodes (μLEDs), as one of potential light sources for the emerging display, have been studied focused on mass transfer, fabrication and efficiency improvement. Degradation of external quantum efficiency (EQE) with size reduction has been considered as an one of challenges hindering the emergence of the μLED display (1). As an origin of the low EQE of μLED, leakage current through defect states distributed around sidewall have been reported. Especially, such trend outstands under 40 μm. During the high-density plasma etching, the high-energy ion induces damage on the sidewall of the LED, resulting in formation of dangling bonds on the surface. These crystal defects function as a serious leakage current path, leading to the EQE degradation (2).

Recently, it was reported that the size effect of green μLEDs differs from that of blue μLEDs, as green μLEDs demonstrate higher external quantum efficiency (EQE) than blue μLEDs at sizes below 10 μm (3). For the green μLEDs, the active layer contains higher indium composition compared with blue emission active layer. The high indium composition in the active layer induces severe lattice mismatch and strain leading to the formation of V-defects within the quantum wells (QWs). These crystal defects are one of the most critical issues in epitaxial growth, since the defects, function as Shockley-Read-Hall (SRH) non-radiative recombination centers, significantly degrades quantum efficiency. In contrast, aggressive downscaling of μLEDs rather gives rise to relatively less gradual EQE reduction of high indium-containing green LEDs, compared to blue ones. It was speculated that In-rich clustering of green emission active layer is beneficial in confining electrons and holes injected in QWs and alleviating their lateral diffusion, which consequently suppresses non-radiative recombination at the sidewall of active layer.

Furthermore, piezoelectric fields are generated in the QWs due to internal strain. Hence, the phenomenon, known as the quantum confined Stark effect (QCSE), arises when the internal electric fields deform the QW band edges, resulting in reduced overlap between the wavefunctions of electrons and holes. This QCSE appears more observable due to larger strain from green-emitting QWs. Since the wavelength shift of QCSE has also something to do with the injected radiative recombining carriers, leakage current behavior of blue and green μLEDs will be strongly influence.

Despite the significance of these indium composition related local electroluminescence (EL) and relevant electrical properties of blue and green uLEDs, their systematic investigation remains less explored so far and in demand. In this work, the blue and green μLEDs are prepared to investigate and compare the spatial distribution of EL spectra of μLEDs with few hundreds nanometers. In order to analyze the spatial information of the EL for blue and green μLEDs, confocal scanning microscope is utilized with highly sensitive spectrometer. The EL distribution correlates their luminous efficiency and leakage current behavior. This approach is useful to investigate and analyze the electrical and optical properties of sub-micron LEDs for AR/VR devices.

2. Experimental Details

Blue and green emission epitaxy were grown on 2 inch c-plane sapphire wafers via metal organic chemical vapor deposition (MOCVD). The epitaxial structures consisted of a 3.2 μm undoped GaN layer, a 4.2 μm Si-doped n-GaN layer, 9 periods of 3 nm/10 nm InGaN/GaN MQWs, and a 100 nm Mg-doped p-GaN layer. Blue and green emission LED structures were separately grown by varying In composition. 37×37 μm² LEDs were defined by photolithography and Cl_2-based inductive coupled plasma etching, resulting in mesa formation and electrical isolation between neighboring LEDs. In order to inject current uniformly, an indium tin oxide (ITO) layer of 60 nm was deposited on top of the p-GaN layer by electron beam evaporation. The transparency and conductivity of ITO layer were improved by rapid thermal annealing at 650°C for 1 minute in the air conditions. Cr/Au of 50/250 nm were deposited on both the n-GaN and ITO layers using electron beam evaporation. As a passivation layer to suppress severe leakage current through the sidewall, a SiO_2 of 700 nm was deposited by plasma-enhanced chemical vapor deposition.

A Keithly 2636B was used to obtain the current density versus voltage (J-V) characteristics and provide a voltage and current source on the devices during spatial-resolved EL measurement. The spatial-resolved EL spectra were collected by confocal scanning microscope (Nanobase Xperam S500). Fig. 1 describes the configuration of confocal scanning microscope and schematic of light path. The lights from the device are collected by objective lens and rerouted to a pin hole. This pin hole blocks the out of focus lights and allows only the lights from the focus point to pass. This feature of confocal microscopy provides strictly limited source of light to spectrometer. Eventually, sub-micron scale lateral resolution is achieved.

ISSN 0097-996X/25/5601-0433-$1.00 © 2025

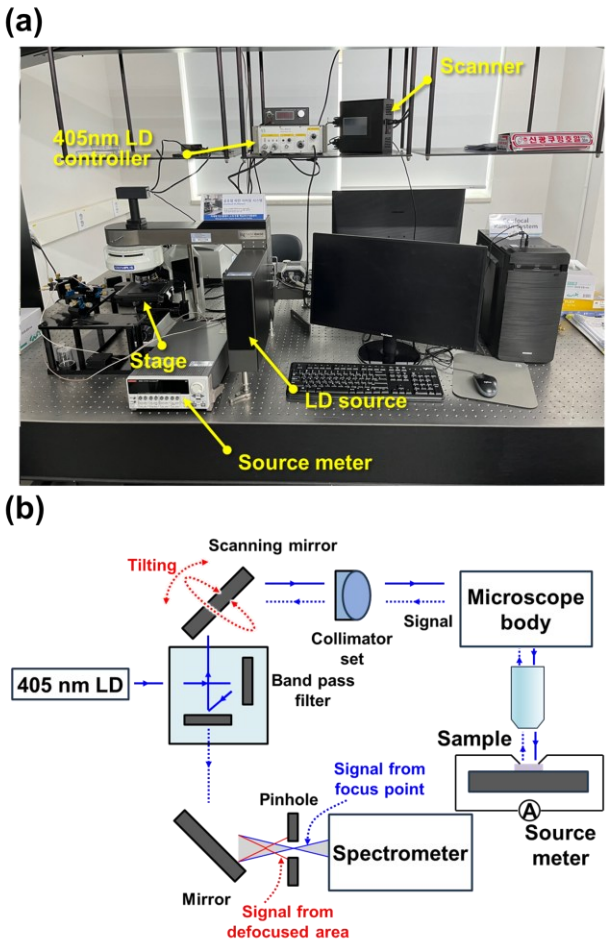

Figure 1. (a) Configuration of the confocal scanning microscopy system and (b) schematic illustrating optical path.

3. Results and Discussion

The J-V characteristics of the blue and green μLEDs were measured along the device sizes in the voltage range 0.5V – 3.5V, as shown in fig. 3(a) and (b). The green μLEDs shows similar current density in the range 1.5 – 2.7 V. However, the blue μLEDs show rise of the current density with chip size reduction in corresponding voltage range. Through the estimation of the current level near the turn-on voltage, it is found that the leakage current behavior differs between blue and green μLEDs. The injected carriers near the turn-on voltage are transported via defect state-assisted tunneling. Notably, the size dependency of the current under low voltage observed in blue μLEDs implies that sidewall leakage current increases with size reduction due to the elevated surface-to-volume ratio. The exposure of GaN to plasma results in the formation of sidewall defects that act as SRH-like non-radiative recombination centers. This phenomenon becomes particularly pronounced when the LED size is reduced. However, the green μLED exhibits unexpectedly no difference in current densities. Such apparent indium composition dependent phenomenon has rarely been reported. Thus, further systematic investigation is necessary to understand the effect of indium composition on μLED performance. Fig. 3(c) shows the applied voltage dependent ideality factor of green and blue μLEDs. The ideality factor is a parameter that represents the extent to which devices adhere to the theoretical current-voltage relationship in diodes. Fig. 2(c) was extracted by the substitution of current and voltage from fig. 2(a) and (b) into the ideal diode equation as follows:

$$n = \frac{q}{kT}\left(\frac{d\ln I}{dV}\right)^{-1} \quad (1)$$

Where q is the elementary charge, k is the Boltzmann constant, and T is the absolute temperature. The minimum ideality factor of the green μLED is calculated to approximately 2. Meanwhile the minimum ideality factor of the blue μLED reaches 3. Two curves for green and blue μLEDs demonstrate relatively stable ideality factor at 1.9 V. Then, the graphs gradually converge in the region III and maintain adherence within the range exceeding 2.4 V due to the increase of the series resistance which can be caused by the joule heating and the current crowding. The fluctuation of the ideality factor in the region I is caused by SRH non-radiative recombination dominant current flow mechanism, considering 1.8 V is closed to turn on voltage. In that region, the energy barrier possibly remains in the energy band structure so that carrier transportation is blocked in between p- and n-GaN. Therefore, only the defect state assisted SRH non-radiative recombination gives rise to the carrier leakage. The area of interest is the region II. The green μLED exhibits the ideality factor of 2, compared to 3 for the blue μLED.

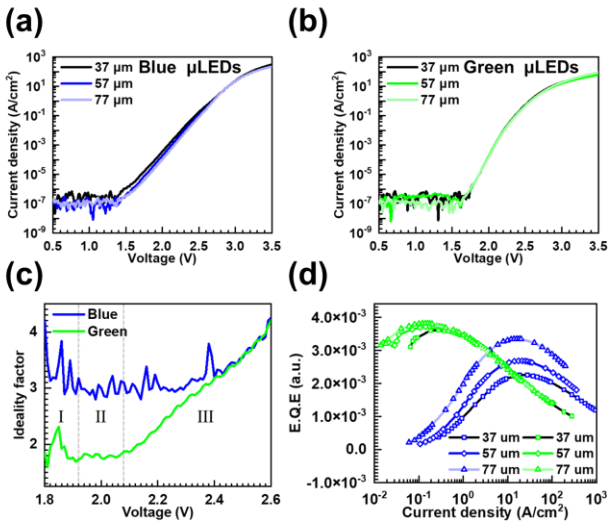

Figure 2. J-V curves for the (a) blue and (b) green μLEDs. (c) Ideality factor in terms of forward voltage for 37×37 μm^2 blue and green μLEDs and (d) external quantum efficiency plotted as a function of injected current density for the blue and green μLEDs of 77×77 μm^2, 57×57 μm^2 and 37×37 μm^2.

Generally, the ideality factors indicate the recombination process and carrier transport mechanisms. The ideality factor of 1 occurs by Sah–Noyce–Shockley (SNS) generation-recombination process and carrier transport processes. Ideality factors above 2 suggest causes of carrier leakage and trap-assisted tunneling. Thus, the blue μLEDs clearly exhibit more severe size effect. Furthermore, this indium composition dependent size effect is confirmed in EL characteristics as shown in fig. 2(d). The light

output is collected in steradians using a photodetector while simultaneously applying voltage to the device for EQE measurement. Fig. 2(d) presents the EQE curves as a function of current density for blue and green μLEDs with dimensions of 77×77 μm², 57×57 μm², and 37×37 μm². The EQE curves for both blue and green μLEDs show an initial increase at low injection levels, reaching their maximum values. As size reduction, the peak current density of the EQE shifts from 13.98 A/cm² to 18.52 A/cm² for the blue LEDs and from 0.12 A/cm² to 0.18 A/cm² for the green LEDs. The difference of the EQE peak current density between large and small μLEDs indicates increase of the A coefficient, in ABC model, corresponding to SRH non-radiative recombination. This is able to be explained as following:

$$EQE = \eta_{inj}\eta_{IQE}\eta_{LEE} = \eta_{inj}\eta_{LEE}\frac{Bn^2}{An + Bn^2 + Cn^3} \quad (2)$$

$$n_{EQE,\max} = \sqrt{A/C} \quad (3)$$

Where η_{inj} is the efficiency of carrier injection to active layer, η_{IQE} is the internal quantum efficiency, η_{LEE} is the light extraction efficiency (LEE), A is the coefficient of SRH non-radiative recombination, B is the coefficient of radiative recombination, C is the coefficient of Auger non-radiative recombination, n is the carrier density, and $n_{EQE,max}$ is the carrier density at EQE peak. When we assume that the LEE, injection efficiency, A, B, and C are constant to the current, $n_{EQE,max}$ can be calculated. Thus, the EQE peak current density shift indicates the increase of the A, considering the order of magnitude of A and C. During the μLED fabrication process, plasma etching creates numerous SRH non-radiative recombination centers at the sidewalls, leading to sidewall leakage currents. It is observed that the maximum EQE points of the blue μLEDs decrease more significantly compared to those of the green μLEDs. This difference becomes particularly pronounced at the 37×37 μm².

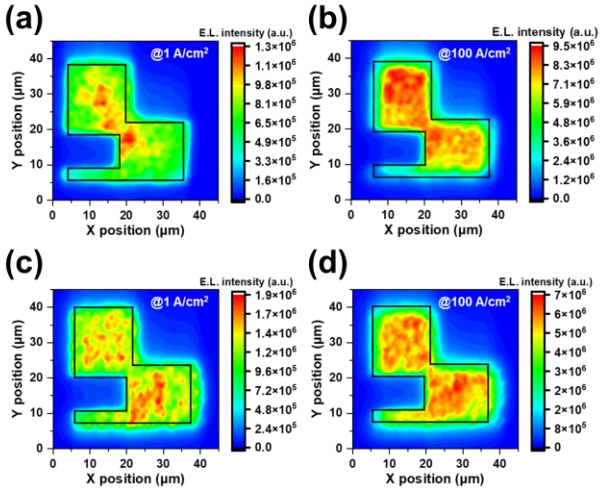

Figure 3. EL intensity mapping for the (a, b) blue and (c, d) green μLEDs at (a, c) 1 A/cm² and (b, d) 100 A/cm², respectively.

Fig. 3 demonstrates the EL intensity map obtained by the confocal scanning microscopy for the 37 μm blue and green μLEDs at 1 A/cm² and 100 A/cm². The configuration of the device is clearly revealed in the blue and green μLEDs with precise dimensional information owing to the features of the confocal scanning microscopy. In terms of the blue μLED, the high intensity spots spread out center to perimeter when the current density rises from 1 A/cm² to 100 A/cm². This spreading out of high intensity area is explained by two reasons: I) severe sidewall leakage current and II) current crowding due to the poor current spreading. However, the distribution of bright regions observed only in the blue μLED. Furthermore, current spreading issues are observed over 40 μm LEDs, as reported in Wong's work (1). On the other hand, the indium composition dependent effect is confirmed in the green μLED by random distribution of the emission spots in the range 1 – 100 A/cm². The high intensity spots of the green μLED appear due to the local deep QWs due to indium aggregation. Comparing with the low indium composition area, the deep QW with high indium content confines more electrons and holes, resulting in high EL intensity.

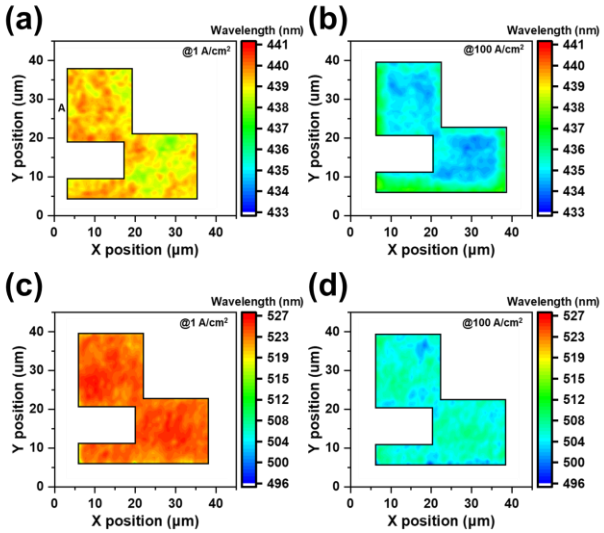

Figure 4. Emission wavelength mapping for the (a, b) blue and (c, d) green 37 μm chips at (a, c) 1 A/cm² and (b, d) 100 A/cm², respectively.

In fig. 4, the graphical representations are redrawn to illustrate emission wavelength. Fig. 4 clearly demonstrates good accordance with the EL intensity map. The emission wavelength indirectly gives information of the carrier injection into the QWs. The wavelength map for the blue μLED has uniform emission distribution at 1 A/cm². When the injection current increases to 100 A/cm², the emission wavelength is shifted to shorter wavelength due to high carrier density in the QWs. Under high current injection, the injected carriers into the QWs recombine and generate photons with not only energy corresponding to band gap, but also higher energy due to band filling effects. Furthermore, carrier induced electric field partially compensates piezoelectric field and lessen band edge bending. Therefore, uniform blueshift is expected to be observed. However, it is found that the longer wavelength emission is located on the perimeter at 100 A/cm². On the contrast, random distribution of emission wavelength appears at 1 A/cm² and 100 A/cm² across the plane area due to carrier localization (3). These results are explained that the deep QWs of the green μLED hinders carrier lateral diffusion and suppresses sidewall leakage current. In terms of the

blue μLED, the injected carriers into the QWs adjacent to the sidewall are transported to the defect states located on sidewall via hopping and tunneling mechanism. Furthermore, green μLEDs contains high density of V-pits with large dimension of which reduce carrier lateral diffusion. During active layer growth, indium atoms are concentrated on the threading dislocation. Thus, deep quantum well and high potential barriers are created around the V-pit edges, as described in a work related to V-pits and leakage current suppression (4).

4. Conclusion

We have investigated InGaN-based blue and green μLEDs, which have different indium composition. The electrical characteristics demonstrate more leakage current at the blue μLED. Furthermore, it is found in the EL map that the strong intensity region spreads out from center to perimeter in the blue μLED. On the other hand, green μLED shows uniform intensity in the EL data. Additionally, correlation between EL intensity maps and EL wavelength maps is found. The EL wavelength maps of the green μLED for 1 and 100 A/cm^2 exhibit uniform EL distribution, while the blue μLED shows gradual spreading out trend of strong intensity region from center to perimeter due to the sidewall effect. In the EL wavelength map, the sidewall effect appears that relatively small changes of the emission wavelength on the edge of the blue μLED, whereas the green μLED has blueshift which is independent on the location. This investigation on the size effect for the blue and green μLED suggests the possible explanation of the differences on the size effect relying on indium composition. We believe better understanding on the size effect leads to the improvement of the μLEDs performance and commercialization of the future display applications such as seamless AR.

5. Impact of Our Research

Nanoscale mappings of EL spectra are demonstrated and correlated with electrical and optical characteristics of micro μLED with different indium contents. By this investigation in depth utilizing confocal scanning microscopy, different appearance of size effect relying on indium contents is revealed. The suppressed sidewall leakage current found in the green μLED provides positive perspective to commercialization of self-emissive complete μLED display.

6. Acknowledgements

Government (MOTIE) and (P0023718, The competency Development Program for Industry Specialist) supported by the National Research Foundation of Korea (NRF) grant funded by the Korea government (MSIT) (No. 2023R1A2C1007034). Additionally, This work was financially supported by Korea Basic Science Institute (National research Facilities and Equipment Center) grant funded by the Ministry of Education.(2021R1A6C101A405).

7. References

1. Wong MS, Hwang D, Alhassan Al, Lee C, Ley R, Nakamura S, et al. High efficiency of III-nitride micro-light-emitting diodes by sidewall passivation using atomic layer deposition. Opt. Express. 2018;26(16):21324.
2. Sugimoto M, Kanechika M, Uesugi T, Kachi T. Study on leakage current of pn diode on GaN substrate at reverse bias. Phys. Status Solidi C. 2011;8(7-8):2512-4.
3. Shin Y, Park J, Bak BU, Min S, Shin DS, Park JB, et al. Investigation and direct observation of sidewall leakage current of InGaN-Based green micro-light-emitting diodes. Opt. Express. 2022;30(12):21065.
4. Kim MK, Choi S, Lee JH, Park CH, Chung TH, Baek JH, et al. Investigating carrier localization and transfer in InGaN/GaN quantum wells with V-pits using near-field scanning optical microscopy and correlation analysis. Sci Rep. 2017;7:1-9.